

Transportable Station for Eye-Safe Laser Ranging of LEO Satellites and Space Debris

Christoph Huber^(1,*), Gerd A. Wagner⁽¹⁾, Frank Schramm⁽¹⁾, Wolfgang Riede⁽¹⁾, and Thomas Dekorsy⁽¹⁾

⁽¹⁾ German Aerospace Center (DLR), Institute of Technical Physics (ITP), Active Optical Systems (AOS), Orbital Photonics Group, Pfaffenwaldring 38-40, 70569 Stuttgart, Germany, ^(*)christoph.huber@dlr.de

Abstract

This paper presents the progress of the Surveillance, Tracking and Ranging Container (STAR-C), developed at the Institute of Technical Physics (ITP) at the German Aerospace Center, for eye-safe laser ranging of LEO objects. It provides an overview of the mechanical improvement that has been made on the lifting platform in order to overcome disadvantages of a movable platform. The paper also shows the specification process of the eye-safe laser system. Current status of STAR-C is presented as well as future plans towards eye-safe laser ranging.

1 INTRODUCTION

The increasing number of space debris objects, ESA's annual space debris report 2023 [1] currently states more than 20,000 objects in low Earth orbit (LEO), and the growth of the satellite population (e.g. mega constellations), lead to the necessity for better collision predictions. Satellite laser ranging (SLR) enables the required accuracy and precision [2] for such high-quality predictions. At the Institute of Technical Physics at the German Aerospace Center a mobile SLR/SDLR station is in development. Its goal is not only to deliver required orbit data but perform ranging measurements with an eye-safe laser. This contribution presents the progress that has been achieved since first presentation of STAR-C at IOC I in 2019 [3].



Figure 1: STAR-C transportable laser ranging system

2 MECHANICAL IMPROVEMENT OF LIFTING PLATFORM

STAR-C is designed to be a mobile platform for SDLR and therefore, uses a lifting platform for its telescope mount. Such a lifting platform, as it is used in STAR-C, has the disadvantage of tilting during operation, when the lifted platform is not completely fixed to the lifting rack [4]. Additionally, there are rubber pads used as dampers instead of pressing the platform directly against the surrounding frame which increases possibility to tilt. Therefore, the platform was modified in order to reduce the tilt.

The idea was to use a latch mechanism which would secure the platform in raised position. Four bolts, two for each side of the platform, were mounted underneath the platform. Their placement is shown in Fig. 2.

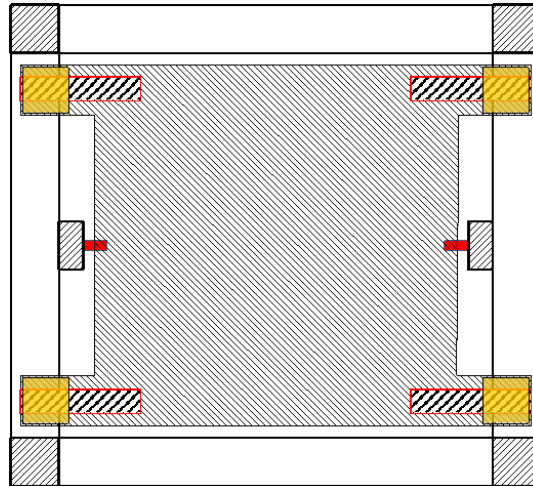


Figure 2: Lifting platform top view [5]

The yellow squares display the attachment points between the platform and the frame. This is also where the rubber pads are located and the latches (red rectangles) are attached to the platform. The bolts are shaped conically the same as the socket holes where the bolts are drive in. Thus, the bolts will center themselves automatically. Not only will this modification reduce tilting due to enhanced rigidity but also ensure that the platform will always return to the same position when lifted.

2.1 Measurements and results

In order to validate the improved platform stability, the high precision inclination sensor from [4] has again been mounted on the lifting platform to measure the inclination of it when the telescope is moving. The two sensor axes (X and Y) were aligned with the long and short sides of the STAR-C container, respectively. Three measurement runs have been performed for the latch mechanism being open and locked. Each time the telescope carried out one full azimuthal rotation. The results are displayed in Figure 33a-d.

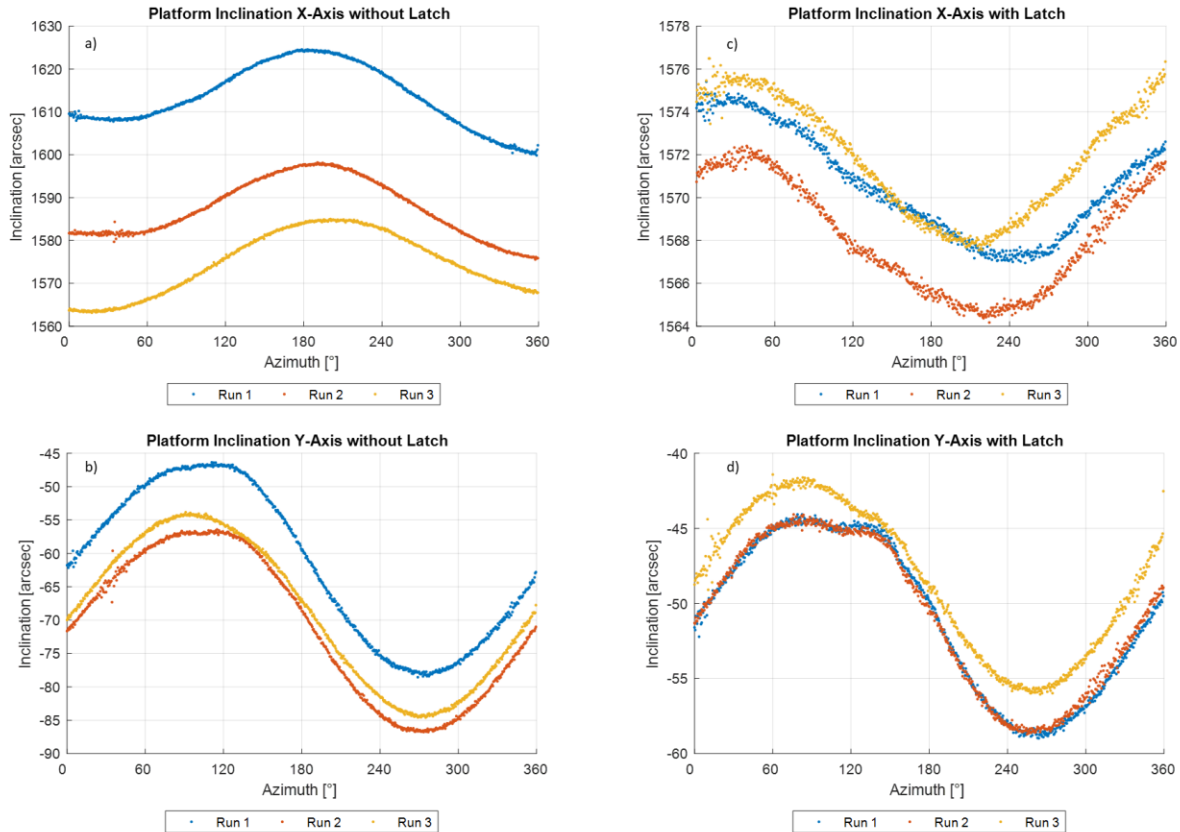


Figure 3: Measurements of the inclination of the lifting platform [5].

Figure 33a and b show the inclination in arcseconds along the container (a) and across (b) with the latch mechanism opened. Clearly visible in both axes is the dependence of the inclination on the azimuthal position of the telescope, with a much stronger expression in the Y-axis. What also can be seen, this only applies to the X-axis, is that the platform doesn't return to the initial inclination after the full rotation has been carried out. This effect is observed in all three measurement runs and indicates an undesirable hysteresis. Furthermore, each measurement shows a similar effect in tilt when rotating the telescope which is also not reproducible. This is attributable to rubber pads. When they get heated up, what is to be expected on a sunny day as it was during measurement, they will get softer over time and therefore, initial contact pressure is getting reduced.

Figure 33c and d display the results when latch mechanism is closed. Still, one can see the same movement pattern but with a much smaller overall extend. Table 1 shows the overall values when latch is open and closed.

Table 1: Measurement of lifting platform inclination with and without latch mechanism

	Run	X-axis			Y-axis		
		1	2	3	1	2	3
Latch open	Mean [arcsec]	1613.52	1587.34	1574.75	-61.75	-70.92	-68.77
	Variance [arcsec ²]	52.06	46.00	51.84	128.39	115.07	111.08
Latch closed	Mean [arcsec]	1570.56	1568.16	1571.87	-50.89	-50.80	-48.42
	Variance [arcsec ²]	5.97	6.59	7.17	26.16	24.70	22.93

Comparing the mean value of the platform inclination one can see that there is quite a variation between each measurement run when the latch is left open. For the X-axis it varies between 1574 and 1613 arcseconds on the Y-axis between -61 and -71 arcseconds. That is a difference of about 40 and 10 arcseconds. This reduces to 4 and 2 arcseconds respectively when the latch is closed. This is an indicator that the platform position is now much more reproducible.

The variance, which can be seen as an indicator how stable the platform is during movement of the telescope decreases by nearly one order magnitude in both axes. This means that the platform tilt during operation is furthermore minimized.

3 CURRENT SETUP OF STAR-C

Since first presentation of STAR-C at IOC I in 2019 [3] has seen several improvements. First, mechanical stability has been improved (see Ch. 2). Second, the laser setup has been modified. The Nd:YAG laser [6] has been revised and is now operating stable at a maximum pulse energy (34 mJ) which still is sufficient for SDLR. Previously, the maximum pulse energy was 50 mJ.

In Fig. 4 the current optical setup is displayed. The 1064 nm laser system (blue) has been supplemented by a 633 nm HeNe laser (guided via fiber F). This was done for easier alignment of the Coudé-path. A half-wave plate and a Glan-Laser polarizer (GLP) are used to set transmitted pulse energy. A beam dump (BP) dissipates excessive energy. A photo diode (PD) triggers data acquisition.

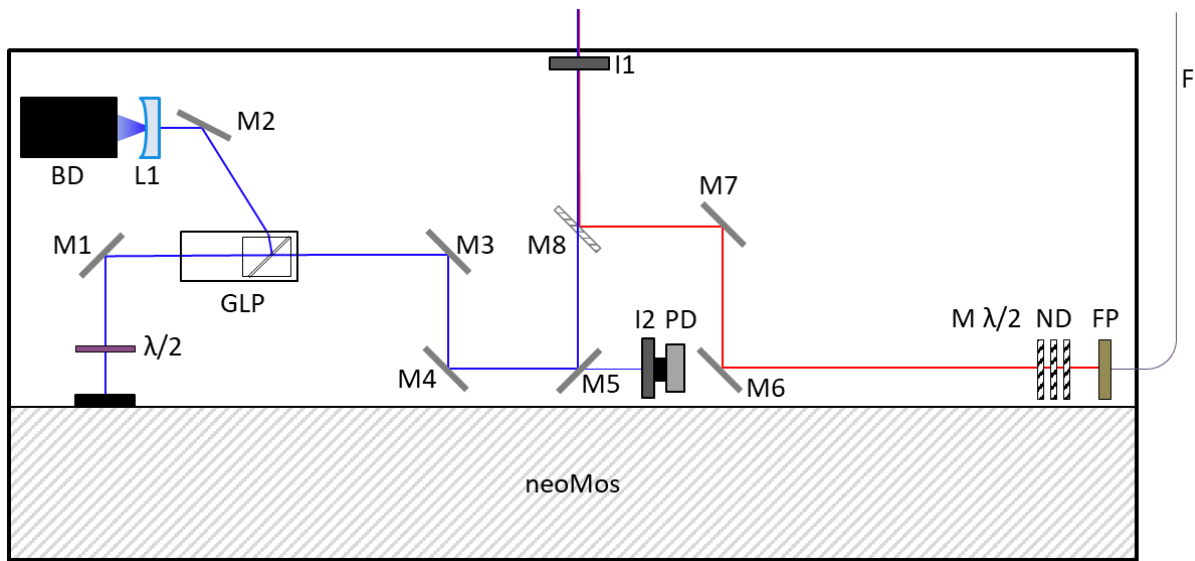


Figure 4: Optical beam path for laser systems at 633 nm and 1064 nm.

Neutral density filters (ND) reduce optical power of the HeNe to eye-safe level. Mirrors (M6-8) are used to guide the laser beam into the Coudé-path inside the telescope mount (not shown) and to the transmitter. Mirror M8 is removable in order to be able to switch to the Nd:YAG laser (neoMos). Pinholes (I1, second inside telescope mount) are used to align neoMos with the pre-aligned Coudé-path. That way only minor adjustments have to be done.

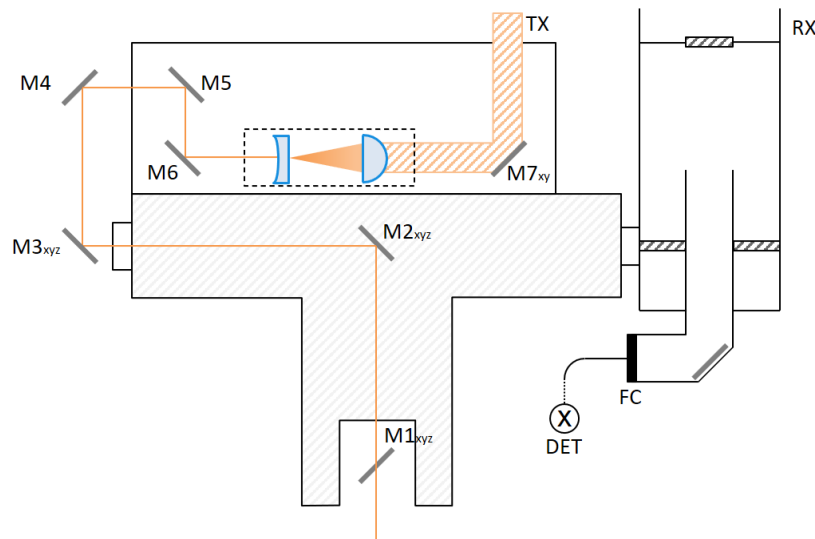


Figure 5: Optical beam path inside telescope mount and transmitter.

Figure 55 shows STAR-C's transmitter and receiver setup. The laser is guided through the telescope mount to the transmitter stage where it is enlarged to 2 inches in diameter. Mirror M7 is the final transmitting mirror. On the right-hand side, the receiving CDK17 telescope is shown where returning photons are collected and guided by a fiber to the detector.



Figure 6: PlaneWave CDK 17 optical tube assembly with attached finder telescope.

In Fig. 6 STAR-C's latest extension is shown. Attached to the receiver telescope is now a 4 in. finder telescope. Paired with the camera EXPLORE SCIENTIFIC [7] it provides a FOV of 2.2 x 1.7 degrees. This will be used as guidance assistance if the object trying to be tracked is not within the FOV of the receiver telescope.

4 CHARACTERIZATION OF 1645 nm LASER SYSTEM

The goal of STAR-C is to perform eye-safe SDLR. Therefore, a new laser system has been acquired. The IPG Photonics ELPN-1645-15-50-15 is a fiber laser pumped solid state laser operating at 1645 nm. Full laser specifications are provided in Tab. 2.

Table 2: IPG Photonics ELPN-1645-15-50-15 specifications

Parameter	Specification
Wavelength [nm]	1645
Maximum average power [W]	17.5
Maximum pulse energy [mJ] (typical)	17.5
Pulse duration [ns] (typical)	75
Repetition rate [kHz]	1-2
Beam diameter [mm]	1.8
Line width at FWHM [nm]	0.09

Prior to planned integration into STAR-C, the laser was fully specified in the laboratory. A power measurement as well as the determination of pulse duration has been performed. Additionally, beam

quality and divergence of the beam have been determined since they were not known before. All measurements have been done at a pulse repetition rate of 1 kHz.

4.1 Power and pulse length measurement

For the power measurement the power meter Nova II by Ophir has been used. The result is shown in Fig. 7. At around 32 W of total pump power the laser is starting to emit. The pulse energy amounts to about 2.8 mJ.

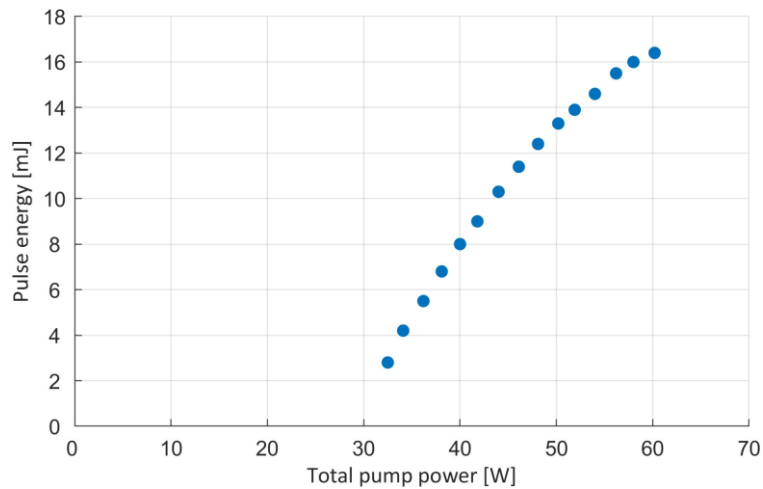


Figure 7: Pulse energy vs pump power of IPG laser.

Raising pump power pulse energy increases as well. Maximum pulse energy is reached at maximum pump power of 60.2 W and amounts to 16.4 mJ.

The measurement of the pulse duration has been done simultaneously using an InGaAs detector (Thorlabs DET10C) and an oscilloscope (Teledyne Lecroy Wavesurfer 3104z).

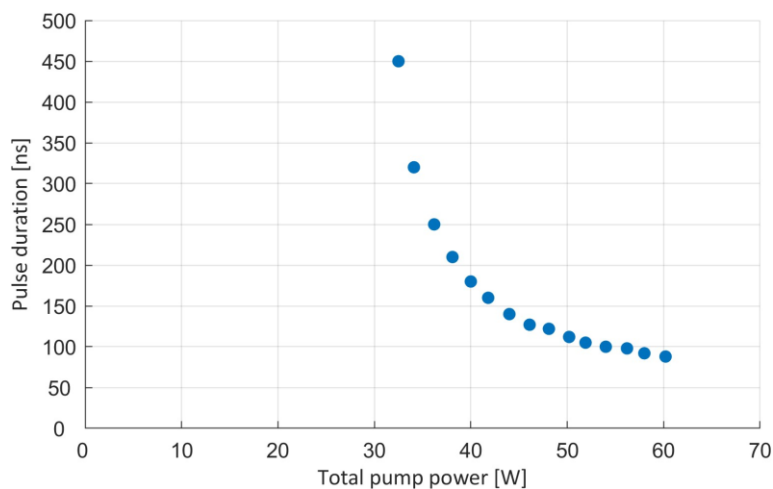


Figure 8: Pulse duration of IPG laser.

Figure 88 shows the pulse duration in ns plotted against the total pump power in W. When the laser starts to emit the pulse duration is rather long (~450 ns) but starts to decrease fast. At maximum pump power the pulse duration amounts to 88 ns which is well within specs.

4.2 Determination of beam quality and divergence

Beam quality and beam divergence are important parameters in laser ranging. High beam quality allows strong focusing of the laser beam while it is important to know beam divergence in order to set the laser spot size in orbit.

The beam quality and the divergence have measured using a M^2 measurement system (Thorlabs M2MS-BP209-IR2/M). Figure 9 shows the setup that has been used for the measurement.

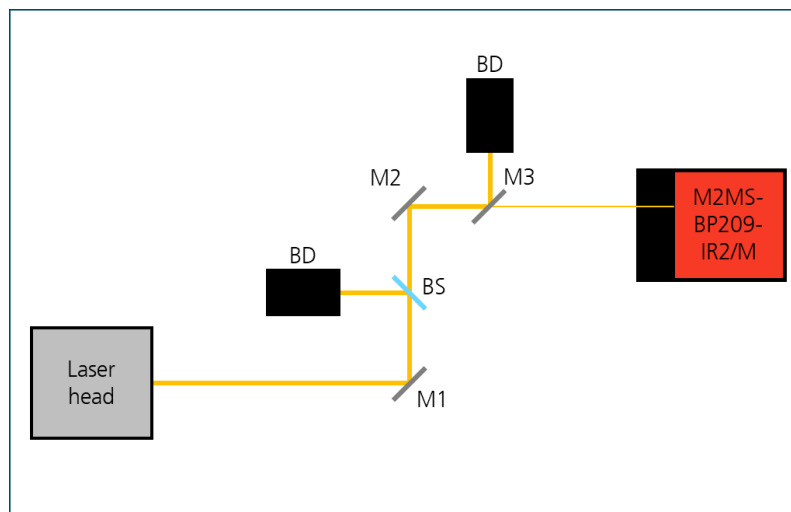


Figure 9: Schematic of setup for measurement of M^2 and beam divergence.

The laser head is placed on the left-hand side. Two mirrors (M1,2) are used for beam walking. During measurement the beam has to hit the profiler in the same spot and under the same angle all the time. Therefore, it is necessary to be able to adjust beam position and angle. A beam splitter (BS) and a third mirror (M3) are used to reduce pulse energy that reaches the detector (damage threshold of detector). The excessive pulse energy is dissipated in beam dumps (BD).

Table 3: Measured laser beam parameters

Parameter	X-axis	Y-axis
M^2 [-]	1.04	2.41
Divergence [mrad]	9.00	11.87

The system is able to perform all measurements automatically with the exception that it only works for cw and quasi-cw laser systems. Therefore, the measurement and calculation has been done manually in accordance to ISO 11146. The results are shown in Tab. 3. The 1645 nm laser has a M^2 of 1.04 and 2.41 in X- and Y-axis, respectively. The divergence amounts to 9.00 and 11.87 mrad.

5 CURRENT STATUS

At the moment, STAR-C is equipped with the 1064 nm laser system (see Ch. 3). Using this laser first atmospheric backscattering measurements have been done in order to test complete system functionality. Before ranging tests to LEO are conducted, the tracking performance of the telescope mount is currently being specified.

6 SUMMARY AND OUTLOOK

Major improvements on lifting platform stability have been achieved. Raised platform position is now highly reproducible and tilting during telescope movement has been drastically reduced. Alignment of the Coudé-path (laser transmitter) has been verified and overall system operation has been tested by using atmospheric backscatter measurements.

The eye-safe laser has been fully specified in the lab. Beam quality and divergence have been determined as well as laser pulse energy and pulse duration. It is now planned to integrate the system into STAR-C. First ranging measurements will provide overall detection limit of the system. Also, it is planned to determine detection limit of the STAR-C system.

REFERENCES

- [1] ESA Space Debris Office. "ESA's Annual Space Environment Report," 2023.
- [2] Degnan, J. J. "*Millimeter accuracy satellite laser ranging: a review*" Contributions of Space Geodesy to Geodynamics: Technology, Vol. 25, 1993.
- [3] Wagner, G. A., et al. "*Mobile Station for Orbit Determination of Satellites and Space Debris*", Proceedings of the International Orbital Debris Conference, IOC 2019.
- [4] Hasenohr, T., et al. "*STAR-C: Towards a transportable Laser Ranging Station*" Proceedings of the International Astronautical Congress, IAC 2017.
- [5] Huber, C., "*Development and specification of a transportable SLR/SDLR station for LEO objects*", Master thesis, University of Stuttgart 2021.
- [6] NeoLASE, Available at <https://neolase.com/en/>, accessed October 2023 .
- [7] Bresser EXPLORE SCIENTIFIC Deep Sky Astro Kamera 16MP, Available at <https://www.bresser.de/en/home/>, accessed October 2023